STELLAR OCCULTATION MEASUREMENTS OF NIGHTTIME OZONE BETWEEN 42 KM AND 114 KM ALTITUDE

G. R. Riegler

Jet Propulsion Laboratory
Pasadena, California 91103

S. K. Atreya, R. J. Cicerone, and S. C. Liu

Department of Atmospheric and Oceanic Science
The University of Michigan, Ann Arbor, Michigan 48109

J. F. Drake

Lockhead Palo Alto Research Laboratory
Palo Alto, California 94304

Proceedings of the Joint Symposium on Atmospheric Ozone of the International Association of Meteorology and Atmospheric Physics and World Meteorology Organization, held in Dresden, G.D.R., August, 1976.

STELLAR OCCULTATION MEASUREMENTS OF NIGHTTIME EQUATORIAL OZONE BETWEEN 42 km AND 114 km ALTITUDE

Guenter R. Riegler, Sushil K. Atreya, Ralph C. Cicerone,

Jerry F. Drake and Shaw C. Liu

ABSTRACT

The Princeton University Ultraviolet Spectrometer-Telescope on the NASA Orbiting Astronomical Observatory 3 was used for stellar occultation measurements of atmospheric ozone. Intead of the usual limb-crossing geometry, this observation used a limb-grazing technique which yielded a higher statistical accuracy for the absorption measurements.

Two sets of observations of β Cen were carried out on 26 July 1975 and 13-14 June 1976 at wavelengths from 2550 to 3100 A. After unfolding of the absorption data, ozone density profiles near the equator within 3 hours of local midnight were obtained at altitudes from 42 km to 114 km. In the lower half of this altitude range, the ozone densities measured in 1975 and 1976 agree with theoretical calculations and one measurement carried out in 1971. Ozone densities in the upper half of this altitude range show a significant excess over the extrapolated low-altitude profile near 100 km, clearly visible in both the 1975 and 1976 data.

A discussion of the statistical and systematic accuracy of the present results, and a comparison with published ozone density profiles is given.

1. INTRODUCTION

The occultation technique for measurements of atmospheric species has been used by a number of researchers to probe planetary atmospheres.

Light from the sun or other stars was measured in certain time intervals while the line-of-sight traversed a varying portion of the atmosphere of the earth or other planets. The resulting variations in recorded counting rate can be converted easily into a measurement of the column density; after further unfolding by a number of methods, an actual density profile is obtained.

Section 2 contains a description of our stellar occultation measurements and the instrument used. An evaluation of the accuracy of the calculated density profiles is presented in Section 3. The results of two sets of ozone measurements are given in Section 4.

2. DESCRIPTION OF INSTRUMENT AND OBSERVING PLAN

Stellar occultation measurements of atmospheric ozone and other constituents were carried out with the Princeton University Ultraviolet Telescope-Spectrometer on the NASA Orbiting Astronomical Observatory OAO-3 Copernicus. The orbit of OAO-3 is nearly circular with 745 km altitude and 35° inclination. These orbital parameters are very favorable for occultation measurements since they permit long occultation times during each orbit, and also reliable long-term predictions of suitable future occultation times.

The OAO-3 star tracker is programmed to track on a portion of the light entering the telescope; another portion is split off to the UV spectrometer. Since the star tracker uses visible light and the spectrometer senses UV light, refraction effects and possible guidance problems limit the range of occultation geometries to tangent altitudes above 30-40 km.

In the usual applications of the occultation method, the line-of-sight to the star crosses the limb of the earth during a time interval of approximately 10 to 25 seconds depending on the satellite orbit and the atmospheric species observed. We are using an observing geometry in which the line-of-sight grazes the earth's limb without actually being occulted by the disc. Typical observing times for this approach are 200-300 seconds, with a corresponding increase in the statistical accuracy of the observation.

The above-mentioned star tracker design also restricts occultation measurements to nighttime observations when the point of minimum tangent altitude (i.e., the "tangent point") is within three hours of local midnight. These restrictions and some engineering constraints limit applications of the limb-grazing method from OAO-3 to one or two observations per star per year.

The minimum tangent altitude during each orbit varies by approximately 10 km per orbit because of the precession of the ascending node of the OAO-3 orbit. This means that the observing wavelength for each orbit must be selected to optimize absorption by atmospheric ozone, i.e., to obtain optical depths between 0.03 and 5. This range of optical depths was selected to minimize the effects of uncertainties in the background and unattenuated counting rates (see Section 3). An observation therefore consists of a sequence of orbits with overlapping altitude ranges and usually different observing wavelengths between 2550 A and 3428 A (the upper wavelength limit for the OAO-3 UV Spectrometer).

Table 1 contains a summary of the 1975 and 1976 measurements of atmospheric ozone. Although the actual data collection during each orbit extended over 240 seconds (limited by the on-board data storage capacity for the observations discussed here), Table 1 lists only the beginning and end of the interval during which the optical depth for absorption along the line-of-sight was between 0.03 and 5. The 1975 measurements were carried out within 25 minutes of local midnight at the tangent point, while the 1976 measurements extended over the range from 0100 to 0300 hours local time.

3. DATA ANALYSIS

3.1 Calculation of Ozone Column Densities

A typical set of data is shown in Figure 1. The histogram on the lower half of the figure shows the counting rate recorded as a function of time, varying from the unattenuated stellar flux value through partial attenuation by atmospheric ozone to the cosmic-ray induced background counting rate and complete absorption of the stellar flux signal.

Using the one-standard-deviation value as a measure of the statistical accuracy, Figure 1 shows that the observed counting rates in each 15-second interval have an accuracy varying from 0.47% to 1.2%.

The calculation of column densities from the relative attenuation of the net stellar flux signal is easily obtained after compensation for the small effect of Rayleigh scattering. Since the bandpass of the OAO-3 Ultraviolet Spectrometer is narrow, typically 0.06-0.08 A, integration over a finite wavelength band is not necessary.

For the conversion from optical depth to column density we have used the ozone absorption cross sections tabulated by Ackerman [1]. According to a review presented by Hudson [2], these absorption cross sections can be assumed to have an absolute accuracy of better than 5%.

Figure 2 shows the resulting ozone column densities as a function of tangent altitude for the July 1975 observations. The data from three orbits for near-equatorial tangent points are shown in this figure. The relative statistical uncertainty of the calculated column densities is indicated when it exceeded 10%. As shown in Table 1, the three sets of data were obtained during three successive orbits, approximately 100 minutes apart, with three different wavelength settings. Near 62 km the three sets of data agree to within better than 10%, while a spread of almost 70% is observed near 50 km.

Ozone column densities calculated from the June 1976 observations are shown in Figure 3. These more recent data (compare Table 1) show a higher level of consistency among the various sets of measurements; the spread between column density values is less than 30% between 42 km and approximately 75 km tangent altitude.

For ease of comparison, the data from the July 1975 observation (Figure 2) have been repeated on Figure 3. It is apparent that the averages of the two sets of measurements never differ by more than approximately 40% in the altitude range from 42 to approximately 75 km.

Figure 4 shows the ozone column densities in the altitude range from 75 to 114 km. The July 1975 observation (Orbit 4 only), represented by the broken line, follows a typical exponential up to approximately 85 km and then exhibits a pronounced maximum near 95 km tangent altitude. Above 105 km, a near-exponential decrease is observed again. The June 1976 data from four orbits show the same feature as the July 1975 data, except that the whole profile appears to be shifted to lower altitudes by 3-5 km.

3.2. Calculation of the Ozone Density Profile

The relation between the line-of-sight column density and the local ozone density is given by the Abel integral which can be readily inverted. For computation purposes it is necessary to first obtain local fits to the column density profile, using quadratic or exponential models (c.f. Roble and Hays [3]) which do, however, introduce local smoothing depending on the number of data points used. This means that the resulting density value at any given altitude is not unique when the set of column densities has a finite spread. Depending on the number of data points used for the local-smoothing calculation, the variation in calculated density values is comparable to, but less than, the percentage spread in the column density values (see Section 3.1).

Figure 5 shows the resulting ozone density profiles for the 1975 and 1976 observations. Both sets of data were treated in exactly the same manner, i.e., at a given altitude range equivalent numbers of data points were used for the local-smoothing calculations. At altitudes below approximately 85 km, the density profile shown in Figure 5 was also verified by a simple Chapman-factor conversion from the column density values; the results were found to be in good agreement with the more élaborate Abel integral inversion.

4. DISCUSSION

A recent theoretical calculation of the range of nighttime equatorial ozone density profiles for a number of plausible reaction rates and solar flux assumptions has been made by S. C. Liu (c.f. Riegler, Drake, Liu, and Cicerone, [4]). This calculated profile is shown in Figure 6 by the upper shaded region. The results of the present set of observations shows adequate agreement with the theoretical model at altitudes up to approximately 90 km. Above this altitude, an unexplained discrepancy between both the 1975 and 1976 observations and the theoretical model exists.

Ozone density profiles obtained by Hays and Roble [5] via the stellar occultation technique in the nighttime equatorial region are also shown in Figure 6. The enhancement seen near 80-85 km altitude appears to be unrelated to the feature seen near 95-100 km altitude in both the 1975 and 1976 observations. Except for the 85-90 km band, where the 1976 observa-

tions agree with the results of Hays and Roble [5], their results appear to be systematically and statistically inconsistent with the data presented here. We are not aware of any published experimental results for altitudes above approximately 90 km.

The results of a March 1971 nighttime equatorial ozone measurement with a rocket-borne chemiluminescent detector by Hilsenrath [6] at altitudes below 67 km are in excellent agreement with the data presented here.

The ozone mass mixing ratio as a function of atmospheric pressure is shown in Figure 7. The "15° North Annual" model of the United States Standard Atmosphere [7] was used as the reference atmosphere.

ACKNOWLEDGEMENTS

This work has been carried out as a Guest Investigation with the Princeton University Telescope on the Copernicus satellite which is sponsored and operated by the National Aeronautics and Space Administration. G. R. R. is a Senior Resident Research Associate of the National Academy of Sciences--National Research Council. This work has been supported by the National Aeronautics and Space Administration under Contract NAS7-100, Task Order RD-65 #261 with the Jet Propulsion Laboratory (G. R. R.), Grant NSG 7187 with the University of Michigan (R. J. C.), Grants NSG 5097 and NSG 5117 with the University of Michigan (S. K. A.), by the National Science Foundation Grant DEF 74-21598 (S. C. L.), and by the Lockheed Independent Research Program (J. F. D.). We acknowledge the use of NCAR computing facilities. The assistance of Dr. E. Barker of Princeton University has been of great help during all phases of this research.

REFERENCES

[1] Ackerman, M., "Ultraviolet Solar Radiation Related to Mesospheric Processes," in Mesospheric Models and Related Experiments, p.149-159, Fiocco, Editor, Reidel, Dordrecht, 1971.

[2] Hudson, R. D., "Absorption Cross Sections of Stratospheric Molecules," Can. J. Chem. 52, 1465, 1974.

[3] Roble, R. G., and Hays, P. B., "A Technique for Recovering the Vertical Number Density Profile of Atmospheric Gases From Planetary Occultation Data," Planet. Space Sci. 20, 1727, 1972.

[4] Riegler, G. R., Drake, J. F., Liu, S. C., and Cicerone, R. J., "Stellar Occultation Measurements of Atmospheric Ozone and Chlorine From OAO-3," J. Geophys. Res., in press, 1976.

[5] Hays, P. B., and Roble, R. G., "Observation of Mesospheric Ozone at Low Latitudes," Planet. Space Sci. 21, 273, 1973.

[6] Hilsenrath, E., quoted in "Observations of the Global Structure of the Stratosphere and Mesosphere With Sounding Rockets and With Remote Sensing Techniques From Satellites," p. 187, in Structure and Dynamics of the Upper Atmosphere, F. Verniani, Ed., Elsevier, Amsterdam, 1974.

[7] U. S. Standard Atmosphere Supplement, U. S. Government Printing Office, 1966.

FIGURE CAPTIONS

Figure 1. A typical set of stellar occultation data from one orbit. A histogram of observed counting rates is drawn in the lower half of the figure. The upper half shows the instantaneous value of the tangent altitude of the line-of-sight and the geographic coordinates of the tangent point.

Figure 2. Ozone column densities below 75 km tangent altitude derived from the 26 July 1975 stellar occultation measurement of β Cen. Data from Orbit 1 (3100 A) are drawn with symbol (•). Orbit 2: 2997 A, symbol (+). Orbit 3: 2825 A, symbol (x). Error bars of one standard deviation length are shown only when the error exceeds 10%.

Figure 3. Ozone column densities below 75 km tangent altitude from the 1975 and 1976 stellar occultation measurements of β Cen. Data from the 26 July 1975 measurements are repeated from Figure 2; Orbit 1: 3100 A, solid line; Orbit 2: 2997 A, dotted line; Orbit 3: 2825 A, broken line. Data from the 13-14 June 1976 measurements are shown for Orbit 3, 3000 A, symbol (x); Orbit 4, 3100 A, symbol (o); Orbit 5, 3000 A, symbol (✱); Orbit 6, 2900 A, symbol (•); Orbit 7, 2700 A, symbol (+). Error bars of one standard deviation length are shown only when the error exceeds 10%.

Figure 4. Ozone column densities above 75 km tangent altitude from the 1975 and 1976 stellar occultation measurements of β Cen. Data from the 26 July 1975 measurements, Orbit 4: 2580 A, broken line. Data from the 13-14 June 1976 measurements are shown for Orbit 7, 2700 A, symbol (+); Orbit 9, 2550 A, symbol (•); Orbit 10, 2550 A, symbol (x); Orbit 11, 2550 A, symbol (o). Error bars of one standard deviation length are shown only when the error exceeds 10%.

Figure 5. Ozone density profiles calculated from the 1975 observations (solid line) and the 1976 observations, symbol (.). See text for a discussion of the inversion calculation.

Figure 6. Comparison of the ozone density profiles calculated from the 1975 observations (solid line) and the 1976 observations, symbol (.) with previous stellar occultation measurements by Hays and Roble (1973; 8.5°N), a rocket-borne measurement by Hilsenrath (1974; 5°N), and a theoretical calculation for equatorial regions presented by Riegler, Drake, Liu, and Cicerone (1976).

Figure 7. Ozone mass mixing ratio as a function of pressure derived from the 26 July 1975 observations (broken line) and the 13-14 June 1976 observations (solid line).

TABLE 1

SUMMARY OF OZONE OBSERVATIONS

Date	26 July 1975				13-14 June 1976							
Orbit Number	1	2	3	4	3	4	5	6	7	9	10	11
Wavelength (A)	3100	2997	2825	2580	3000	3100	3000	2900	2700	2550	2550	2550
Univ. Time[1] (HH-MM-SS)	03-01-57	04-44-42	06-24-19	08-03-08	12-12-41	13-55-11	15-34-48	17-14-09	18-53-46	22-12-44	23-52-05	01-31-42
Tangent Altitude (km)												
Begin[2]	73.8	67.4	75.4	75.4	79.5	63.9	76.4	75.1	101.2	106.8	107.6	108.7
End[2]	48.3	47.6	57.3	113.7	56.2	41.7	48.7	54.6	64.5	84.5	94.7	104.3
Longitude[3], Latitude (°)												
Begin[2]	305.1,+2.2	284.3,+0.4	260.1,+0.1	248.0,-8.0	209.1,+3.2	187.7,+1.0	162.9,+0.9	138.9,+0.3	110.8,+2.3	62.9,+1.0	39.8,-0.1	351.0,-0.8
End[2]	312.0,-1.0	290.8,-3.6	266.5,-3.2	256.5,-12.0	212.5,+1.1	192.7,-2.1	168.8,-2.7	146.6,-4.4	120.9,-3.9	71.3,-4.1	48.7,-3.7	355.2,-3.4

(1) Time for beginning of a 4-minute data recording sequence.

(2) Beginning and end of useful data collecting interval.

(3) Longitude counting positive eastward.

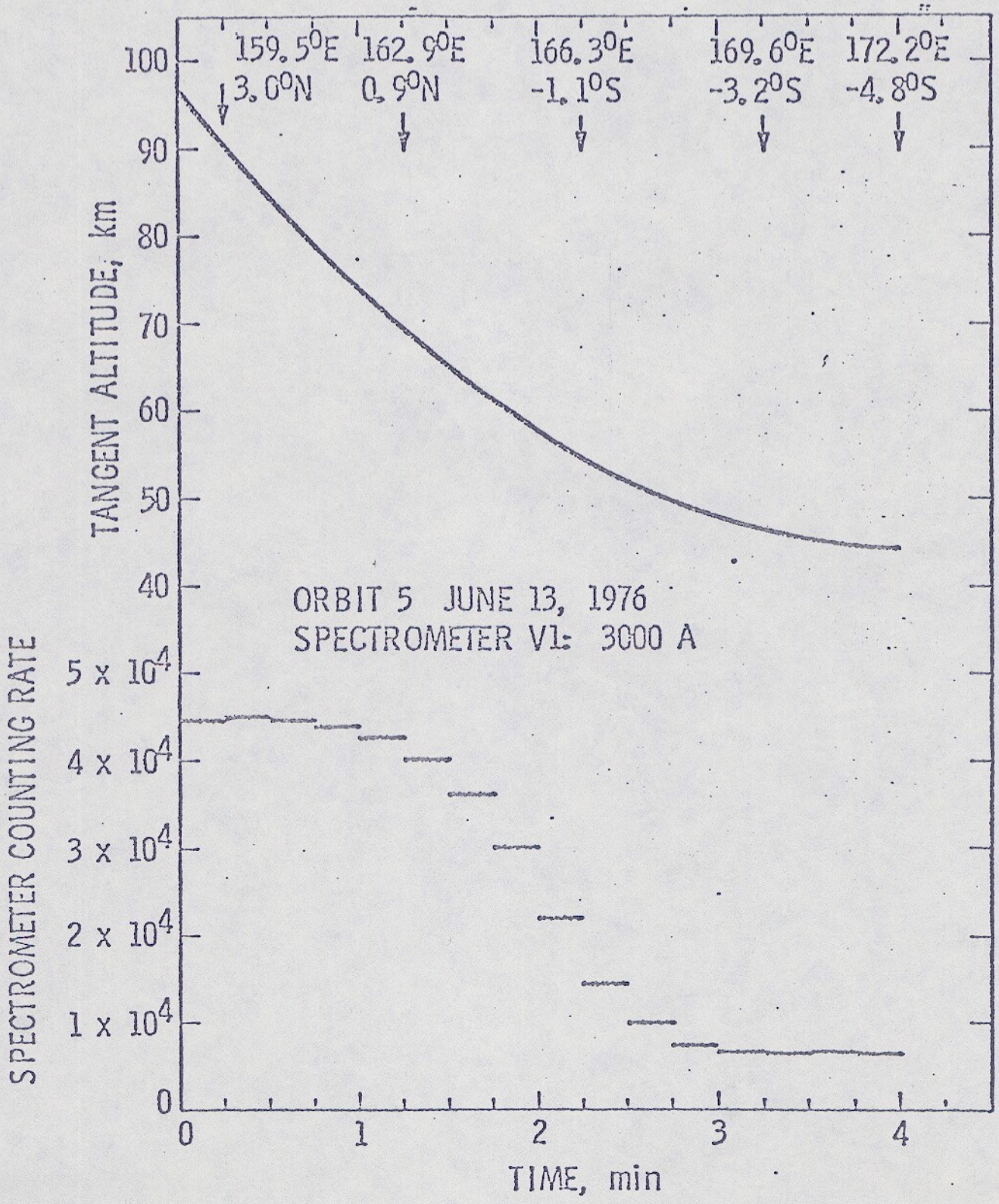
159.5°E 3.0°N
162.9°E 0.9°N
166.3°E -1.1°S
169.6°E -3.2°S
172.2°E -4.8°S
TANGENT ALTITUDE, km
100
90
80
70
60
50
40
ORBIT 5 JUNE 13, 1976
SPECTROMETER V1: 3000 A
SPECTROMETER COUNTING RATE
5 x 10^4
4 x 10^4
3 x 10^4
2 x 10^4
1 x 10^4
0
0
1
2
3
4
TIME, min

Figure 1

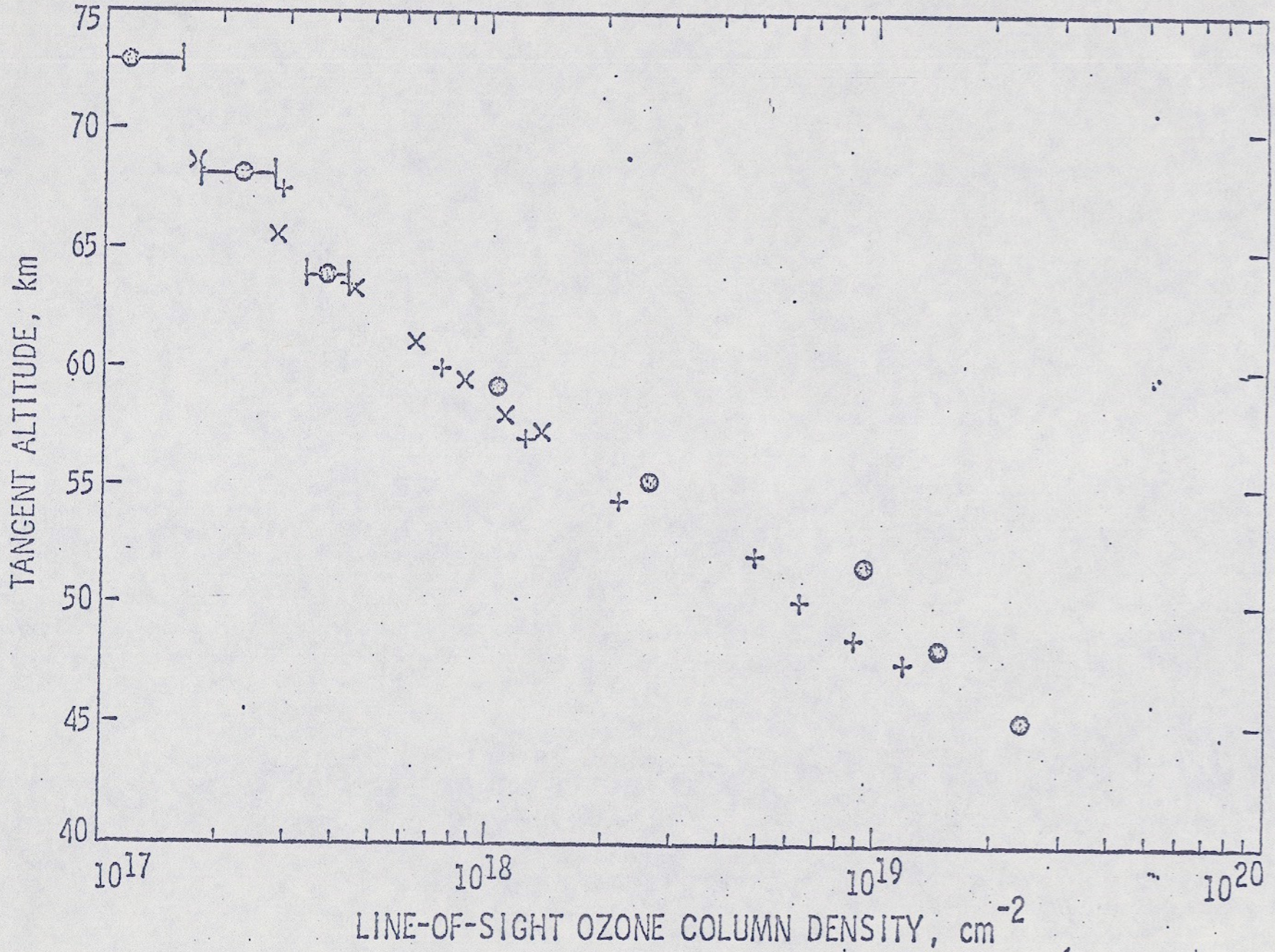
75
70
65
60
55
50
45
40
TANGENT ALTITUDE, km
10^{17}
10^{18}
10^{19}
10^{20}
LINE-OF-SIGHT OZONE COLUMN DENSITY, cm^{-2}

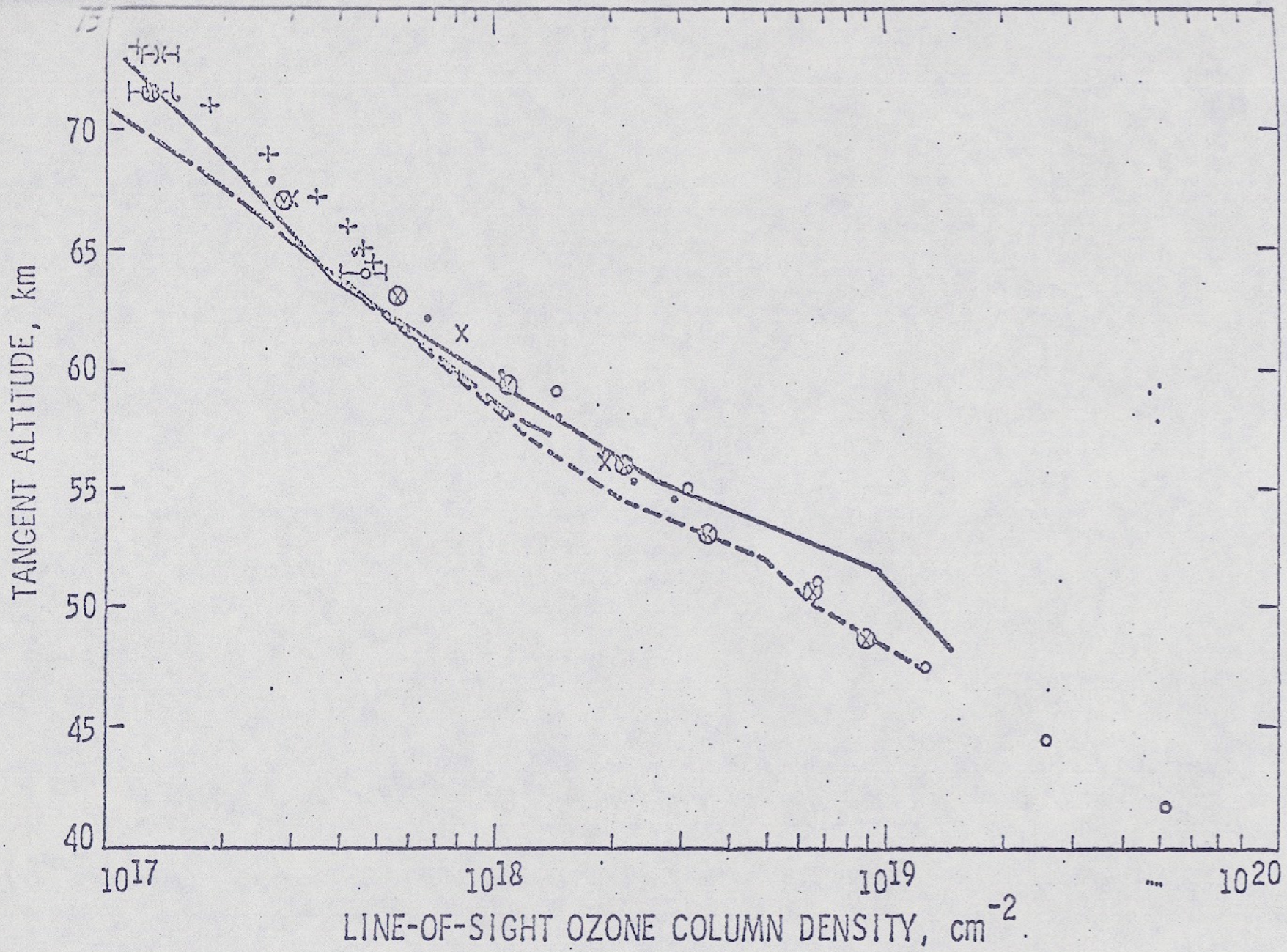
TANGENT ALTITUDE, km
70
65
60
55
50
45
40
10^{17}
10^{18}
10^{19}
10^{20}
LINE-OF-SIGHT OZONE COLUMN DENSITY, cm^{-2}

Figure 3

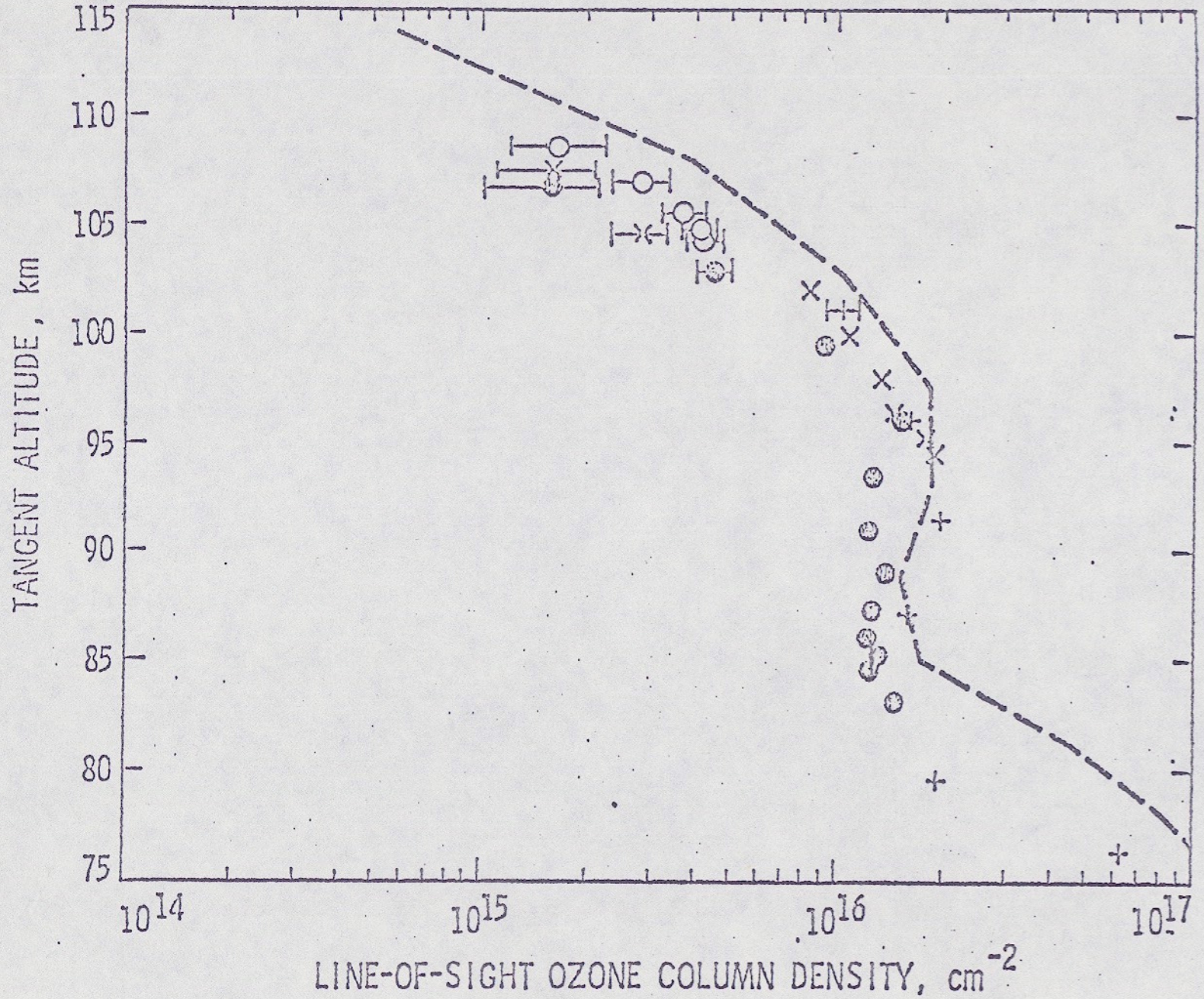
115
110
105
100
95
90
85
80
75
TANGENT ALTITUDE, km
10^{14}
10^{15}
10^{16}
10^{17}
LINE-OF-SIGHT OZONE COLUMN DENSITY, cm^{-2}

Figure 4

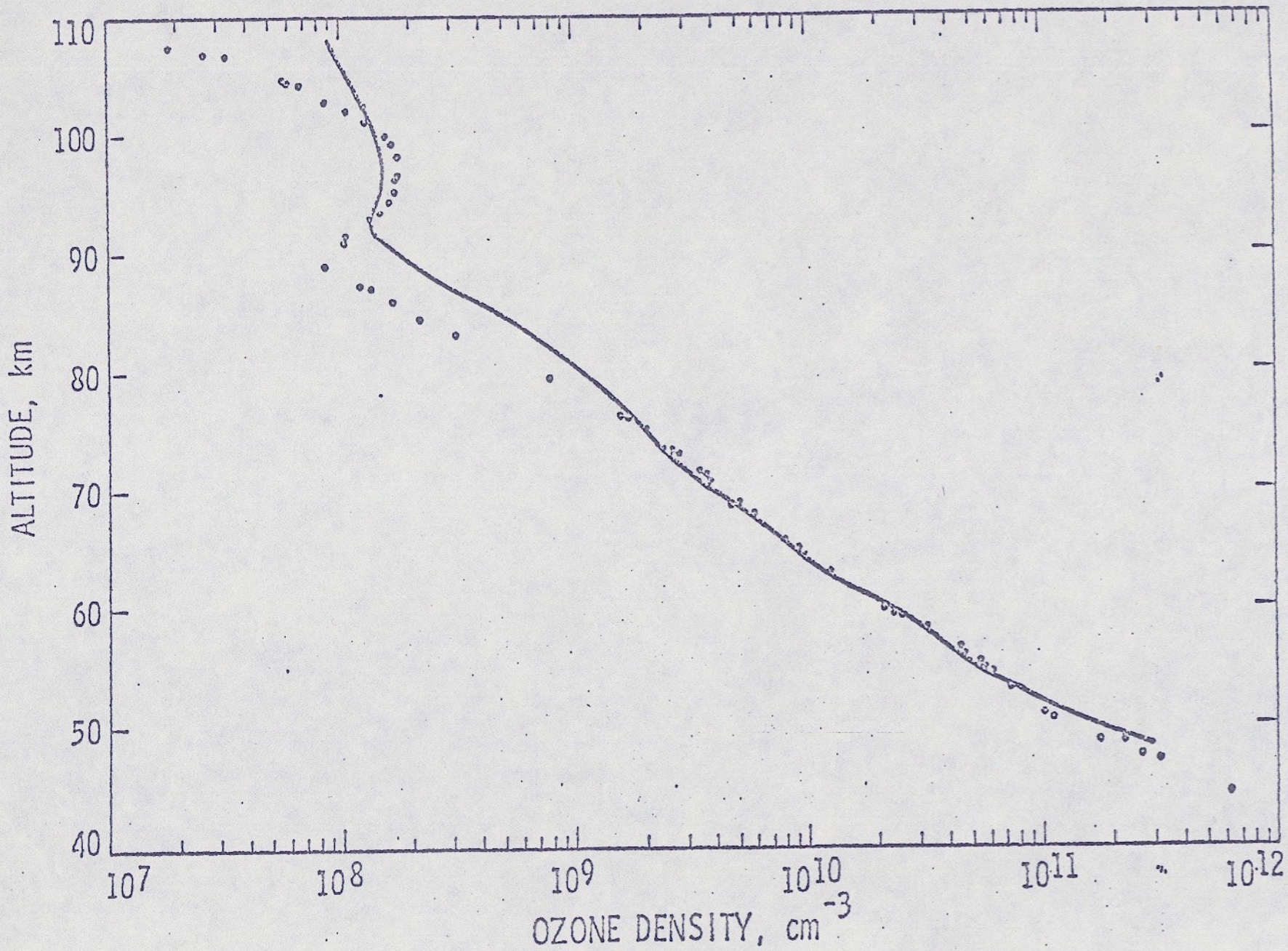
110
100
90
80
70
60
50
40
ALTITUDE, km
10^7
10^8
10^9
10^{10}
10^{11}
10^{12}
OZONE DENSITY, cm^{-3}

Figure 5

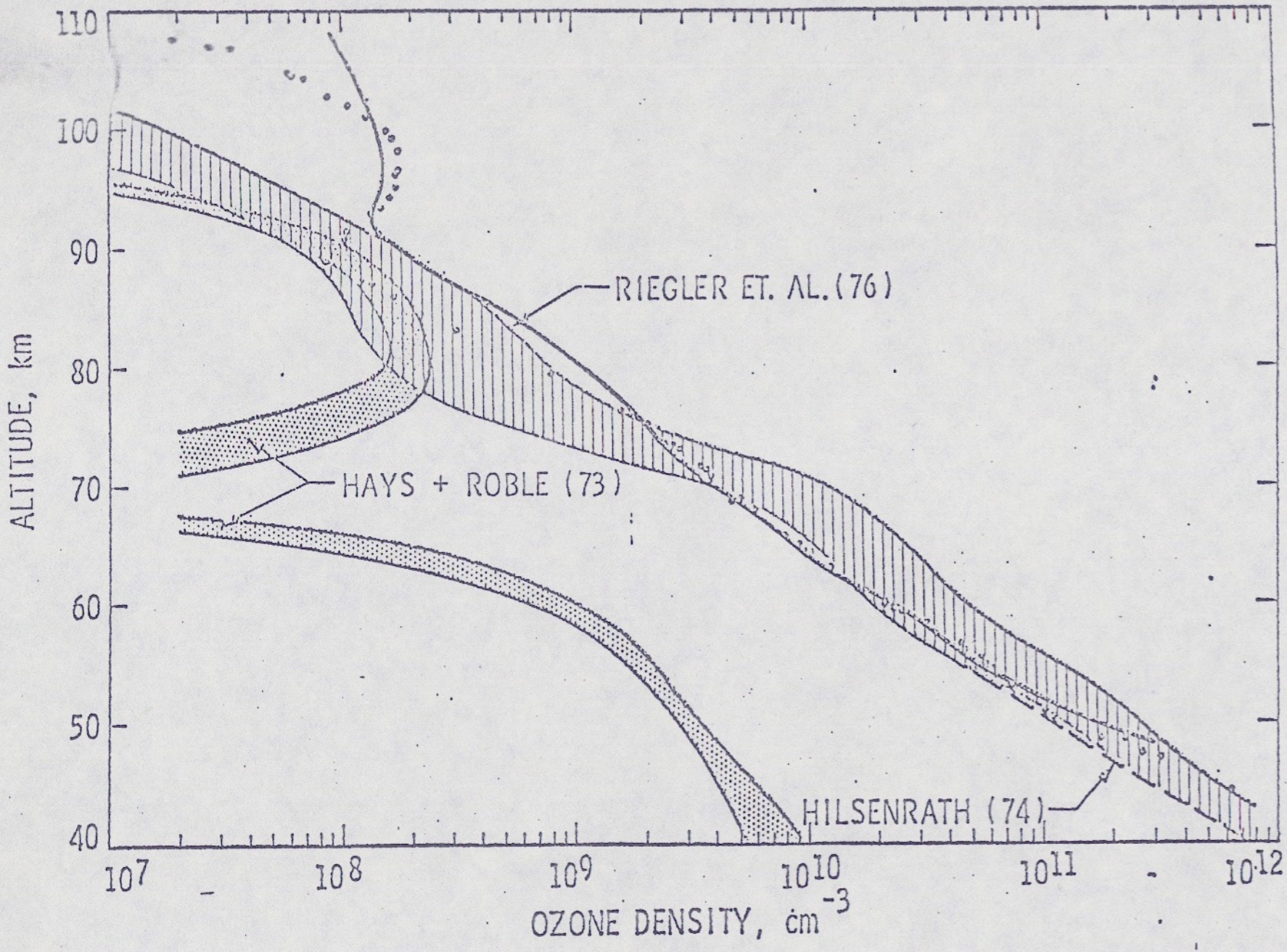
110
100
90
80
70
60
50
40
ALTITUDE, km
RIEGLER ET. AL. (76)
HAYS + ROBLE (73)
HILSENRATH (74)
10^7
10^8
10^9
10^{10}
10^{11}
10^{12}
OZONE DENSITY, cm^{-3}

Figure 6

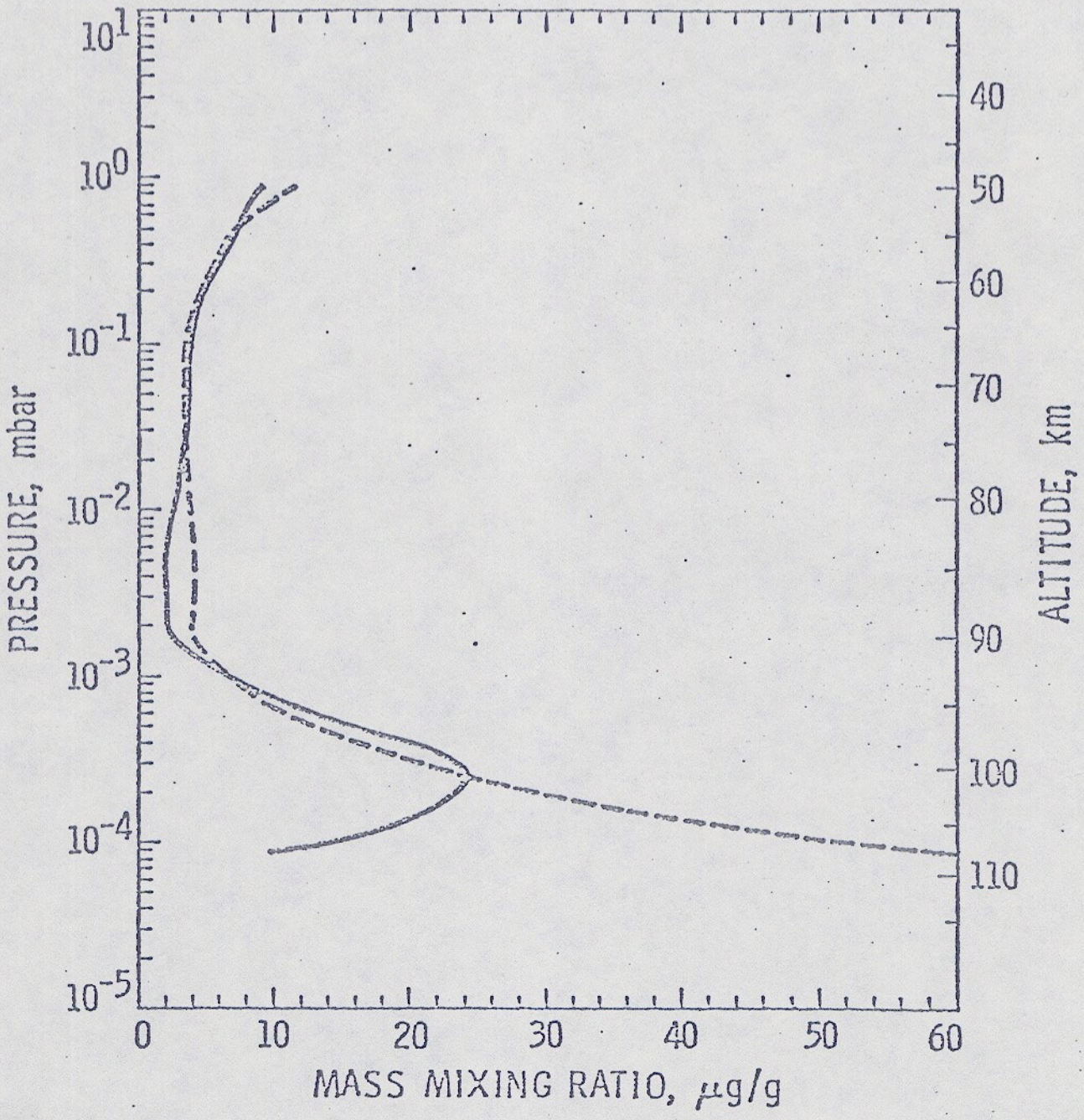
PRESSURE, mbar
10^{1}
10^{0}
10^{-1}
10^{-2}
10^{-3}
10^{-4}
10^{-5}
ALTITUDE, km
40
50
60
70
80
90
100
110
0
10
20
30
40
50
60
MASS MIXING RATIO, μg/g

Figure 7